Chemical Engineering Journal 361 (2019) 209–218

Contents lists available at ScienceDirect

Chemical Engineering Journal

journal homepage: www.elsevier.com/locate/cej

Perchlorate removal from brackish water by capacitive deionization: Experimental and theoretical investigations

Wenle Xing[a,b], Jie Liang[a,b,*], Wangwang Tang[a,b,*], Guangming Zeng[a,b], Xiangxi Wang[a,b], Xiaodong Li[a,b], Longbo Jiang[a,b], Yuan Luo[a,b], Xin Li[a,b], Ning Tang[a,b], Mei Huang[a,b]

[a] College of Environmental Science and Engineering, Hunan University, Changsha 410082, PR China
[b] Key Laboratory of Environmental Biology and Pollution Control, Ministry of Education, Hunan University, Changsha 410082, PR China

HIGHLIGHTS

- The feasibility of perchlorate selective removal by batch-mode CDI was investigated.
- A one-dimensional CDI process model was developed to describe the process.
- A favorably strong preferential adsorption of ClO_4^- over Cl^- was observed.

ARTICLE INFO

Keywords:
Capacitive deionization
Perchlorate removal
Ion selectivity
Theoretical model

ABSTRACT

Capacitive deionization (CDI) has attracted increasing attention over the past decade for the facile removal of ions from aqueous solutions. Nowadays, CDI is rapidly growing and evolving, and has been applied in many aspects. One important application field is water remediation, i.e., removing ionic contaminants of concern from water. Herein, we investigated the feasibility of perchlorate removal from brackish waters by batch-mode CDI technology. Effects of various operating parameters on dynamic electrosorption processes of both perchlorate and chloride were examined. Meanwhile, a one-dimensional CDI process model for dual-anions was developed to quantitatively describe the electrosorption kinetics of perchlorate and chloride, and an excellent agreement between the modeling results and the experimental data was observed. Experimental results revealed a favorably strong preferential adsorption of ClO_4^- over Cl^- in the studied CDI system under various conditions. Moreover, only slight discrepancy between adsorption-desorption cycles was found, demonstrating the good regeneration of electrodes and operational stability of the CDI cell. Finally, the scale-up studies indicated that the CDI stack with multiple pairs of electrodes could achieve a much more superior ion removal performance than the CDI cell with only one pair of electrodes. To conclude, these results showed that the CDI system was effective for perchlorate selective removal in the presence of other major ions and had potential in treatment of perchlorate-contaminated brackish water.

1. Introduction

Perchlorate (ClO_4^-), as the critical national strategic chemical, has been extensively used in the production of propellants for rocket and missile, explosives, fireworks, and automobile airbags [1,2]. ClO_4^- has attracted serious concern due to its chemical stability, high solubility, low adsorption to natural substance and kinetic inertness [3]. ClO_4^- can stably persist in water for many decades [4,5], and high levels of ClO_4^- would have adverse impacts on human health through interfering with iodine uptake into the thyroid gland [6]. Therefore, an official reference dose (RfD) of 0.7 μg/kg/day has been established by the U.S. EPA for ClO_4^- which is equal to the Drinking Water Equivalent Level of 24.5 μg L^{-1} in solution [2]. Although many methods such as adsorption, membrane filtration, ion exchange, biological remediation and chemical reduction have been applied to remove ClO_4^- from water [6–10], these methods suffer from limitations, hindering their practical applications [5]. For example, the biological remediation requires rigorous conditions, and the pathogenic microorganisms might enter into drinking water during biological treatment process and cause potential public health risk [2,11]. The chemical reduction removes ClO_4^- by reducing ClO_4^- to non-toxic Cl^- species, however, it is subjected to low removal efficiency, low catalytic activity to ClO_4^-, and high environmental impacts with eco-toxicity and acidification [5,12].

* Corresponding authors at: College of Environmental Science and Engineering, Hunan University, Changsha 410082, PR China.
E-mail addresses: liangjie@hnu.edu.cn (J. Liang), wtang@hnu.edu.cn (W. Tang).

https://doi.org/10.1016/j.cej.2018.12.074
Received 4 October 2018; Received in revised form 12 December 2018; Accepted 14 December 2018
Available online 15 December 2018
1385-8947/

With key advantages of low energy consumption (i.e., enabling ion removal at room temperatures, low pressures and low voltages with additional possibility of energy recovery), low environmental impact (i.e., without the use of any added chemicals or the generation of hazardous substances) and low investment cost (i.e., simple equipment structure and convenient operation maintenance), capacitive deionization (CDI) has attracted extensive academic and industrial interest as a promising electrochemical water desalination technology for the facile removal of ions from aqueous solutions via electrostatic interactions, especially for desalination of waters with low to medium salinity [13–17]. Generally, a CDI cell is composed of two graphite current collectors and a pair of carbon electrodes (the anode and the cathode) with a separator in-between enabling the feed water to be transported [17,18]. The carbon electrode pair is usually charged with a potential difference smaller than 1.23 V, and salt ions present in the feed are attracted to move towards the electrodes and finally electrostatically retained in the electric double layers (EDLs) at the carbon/water interface, thereby producing a stream of desalinated water [19]. Following ion electrosorption, the electrodes can be regenerated by short-circuiting the anode and cathode or reversing polarity with the trapped salt ions released back to the bulk solution, thereby generating a stream of concentrated water [20,21]. In addition to water desalination, CDI is also being actively explored for remediation of water contamination. It has been reported that CDI is an effective technology to remove ionic contaminants from water, such as nitrate, fluoride, sulfate, phosphate, which exist at low concentrations but have adverse impacts on the environment and human health [22–26]. However, there is no available information about the effectiveness of CDI in ClO_4^- removal. Moreover, considering that, in typical environment scenarios, ClO_4^- frequently co-exist with other electrolytes such as NaCl, it is of great significance to achieve selective removal of target ions (ClO_4^-) in the presence of "major" ions (Na^+ and Cl^-) whose concentrations may be significantly higher than the target ionic contaminants. Consequently, investigating the performance of CDI for ClO_4^- removal in the presence of NaCl represents a meaningful research and is beneficial to the future development and practical applications of CDI.

While CDI clearly has simple structures, it is a complex process depending on a wide range of parameters, such as process parameters, electrode area, electrode and spacer channel thickness, and pore size distribution [27]. Careful selection of operating and design parameters for particular source waters is required. Laboratory investigation of the effects of each parameter on various aspects of CDI performance under different conditions is tiring and cumbersome in view of the difficulty in manipulating some parameters and the interplay between factors. In contrast to experimental study, theoretical model could address this issue nicely and play an important role in quantitative analysis of CDI performance under well-defined configurations and operating conditions [17,24,28]. Apart from enabling optimization of both operating and design parameters, the theoretical model also serves as a useful and essential tool to reveal the underlying causes of phenomena, help to gain thorough understanding of the ion electrosorption process and predict CDI performance in all its facets (e.g., effluent ion concentration, energy consumption, average salt adsorption rate, ion adsorption capacity) [27,29,30].

For these reasons, in this study, we investigated, both experimentally and theoretically, the feasibility of selective removal of ClO_4^- from brackish waters (containing both $NaClO_4$ and NaCl) by CDI technology. Effects of various operating parameters, including applied voltage, initial ClO_4^- (or NaCl) concentrations and pump flow rate, on the dynamic electrosorption processes of both ClO_4^- and NaCl were studied. Meanwhile, a one-dimensional CDI process model was developed to quantitatively describe the electrosorption kinetics of ClO_4^- and Cl^-. Experiments were also conducted to probe into the pH fluctuations, charge efficiency, adsorption-desorption cycling process and the effect of natural organic matter (NOM) on ClO_4^- removal for the purpose of guiding the related CDI practical applications.

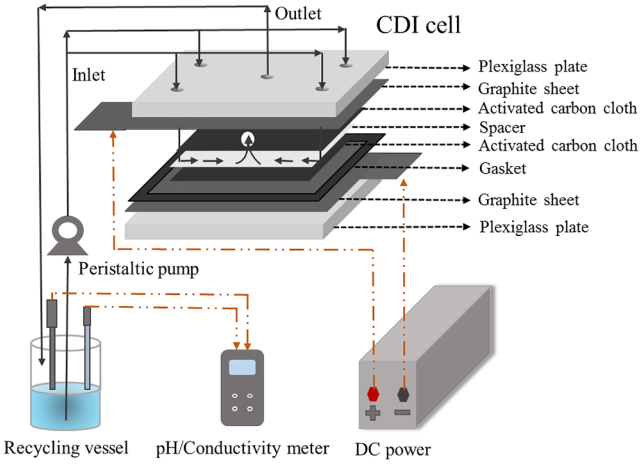

Fig. 1. Schematic diagram of the CDI cell and the experimental set-up.

2. Materials and methods

2.1. Fabrication of CDI device

The CDI cell with one pair of carbon electrodes and the schematic of its configuration are displayed in Fig. 1. The CDI cell is composed of two graphite sheets as current collectors facilitating electron transfer, one pair of activated carbon fiber cloths (10 cm × 10 cm dimension) as binder-free electrodes for capacitive ion sorption and a 200 μm thick non-conductive nylon cloth as spacer channel enabling feed water to be transported from the perimeter to the center of the unit. The graphite sheets were purchased from Heilongjiang Juxiong Import & Export Company Ltd. China with a thickness of 100 μm while the activated carbon fiber cloth was purchased from Nantong Senyou Carbon Fiber Cop. China with a thickness of 300 μm. The specific surface area calculated using the Brunauer-Emmett-Teller (BET) method, grammage and carbon ratio of the carbon cloth are 1118 $m^2 g^{-1}$, 165 $g m^{-2}$ and 89%, respectively. Acrylic end plates with holes drilled around the perimeter to allow for fastening were used to hold together the separate parts. A CDI stack with seven pairs of carbon electrodes in parallel was also constructed for further studies.

2.2. Experimental methods

Electrosorption experiments were carried out in a batch mode as presented in Fig. 1. The system consisted of a recycling vessel, a peristaltic pump (BT-300, Longer Precision Pump Co., Ltd, China), a CDI device, a DC power supply (MS155D, Maisheng Electronic Equipment Co., Ltd, China), a digital electrical conductivity (EC) meter (DDS-307, INESA Scientific Instrument Co., Ltd, China) and a pH meter (PHS-3C, INESA Scientific Instrument Co., Ltd, China). The solution in the recycling vessel was pumped through the CDI device and then flowed back to the recycling vessel. Prior to electrosorption experiments, the CDI device was washed with distilled water at short circuit mode till the conductivity of the water in the recycling vessel was lower than 2 μs/cm, in order to remove external charge and ions remained in the device. Subsequently, the feed solution was prepared in the vessel and was fully mixed with the pure water in the CDI device till the reading of the EC meter became stable. We termed the mixed solution with steady conductivity as the initial solution before charging and its ion concentration as the initial ion concentration. The electrosorption experiments started with a charging voltage applied while the desorption experiments started with a short circuit applied. The solution in the recycling vessel was stirred throughout the test to ensure a homogeneous composition. No pH adjustment was carried out during the whole operation unless otherwise stated. The used chemicals sodium perchlorate

($NaClO_4$), sodium chloride (NaCl), sodium sulfate (Na_2SO_4), sodium bicarbonate ($NaHCO_3$) and sodium hydroxide (NaOH) were of A.R. grade and obtained from Shanghai Chemical Reagent Co. Ltd., China. Solutions of perchlorate, chloride, sulfate and bicarbonate were prepared by dissolving relevant solid chemicals in the ultrapure water. The commercial sodium humate was adopted as model substances representative of natural organic matter (NOM) in natural water bodies. Duplicate runs were carried out for each set of experimental conditions to ensure the accuracy of the measured results. The cell was used for several months of intermittent operation (about 180 cycles in total) with the same set of electrodes used for all the experiments without NOM. When the studies on the effects of NOM were conducted, a new pair of electrodes was used with the performance of the new assembled cell maintaining identical to that of the old one.

Cyclic voltammetry (CV) was conducted to evaluate the capacitive characteristics of the carbon cloth electrodes. CV measurements were performed using an electrochemical analyzer (CHI 627D, CH Instruments, Inc., USA) with a conventional three-electrode cell in 80 mg L^{-1} perchlorate solution at room temperature. The three-electrode cell consisted of a standard calomel electrode as the reference electrode, a platinum mesh as the counter electrode and the carbon cloth electrode as the working electrode. The scan rate was set at 100 mV s^{-1} and the potential range was between −1.2 V and +1.2 V. Steady increase and decrease observed in current with electric potential indicated that no evident oxidation or reduction in sodium perchlorate solution occurred in the selected potential range (Fig. 2).

2.3. Analysis

Water samples were collected from the recycling vessel at appropriate predetermined intervals. After each sample was filtered with 0.22 μm filter membranes, ClO_4^- concentrations were determined using an ICS-900 ion chromatograph (Dionex, USA) equipped with a 500 μL sample loop, a set of AS16 analytical column (4 × 250 mm) and AG16 pre-column (4 × 50 mm) with 35 mM KOH eluent at a flow rate of 1.0 mL min^{-1} while Cl^- concentrations were measured by ion chromatograph (Dionex ICS-900, USA) equipped with an AS23 analytical column (4 × 250 mm) and an AG23 pre-column (4 × 50 mm) with 9.4 mM Na_2CO_3 and 1.8 mM $NaHCO_3$ eluent at a flow rate of 1.0 mL min^{-1}. The samples containing NOM were treated with the pretreatment P column (Qingdao Analysis Lab Science and Technology Co. Ltd, China) prior to being filtered with 0.22 μm filter membranes.

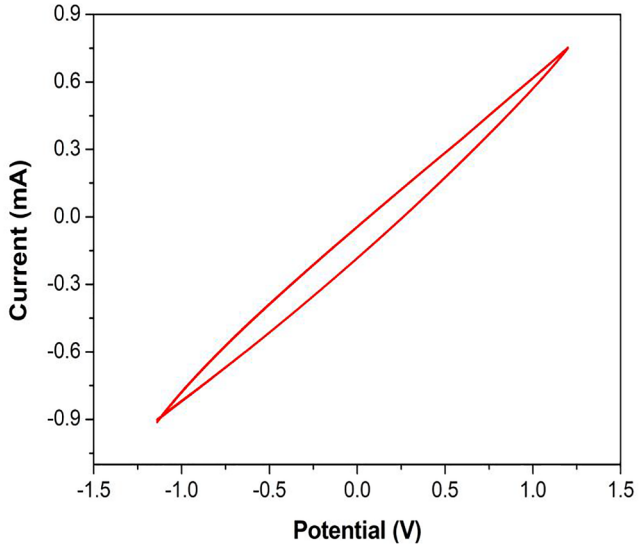

Fig. 2. Cyclic voltammogram for the carbon cloth electrode in 80 mg/L perchlorate solution at a sweep rate of 100 mV/s.

The NOM concentrations were measured by total organic carbon analyzer (TOC-V CPH, Shimadzu, Japan) after each sample was filtered with 0.45 μm membranes.

The electrosorption removal efficiency and adsorption capacity of ion j were calculated as follows,

$$\text{Electrosorption removal efficiency } E_j\ (\%) = (c_{j,0} - c_{j,t}) \times 100/c_{j,0} \quad (1)$$

where $c_{j,0}$ and $c_{j,t}$ (mg L^{-1}) are the initial concentration and the final concentration of ion j, respectively.

$$\text{Adsorption capacity } Q_j\ (\text{mg g}^{-1}) = (c_{j,0} - c_{j,t})V_{tot}/M \quad (2)$$

where V_{tot} is the total water volume (L), and M is the total mass of two electrodes (g).

Ion selectivity between ClO_4^- and Cl^- was calculated according to,

$$S_{ClO_4^-/Cl^-} = E_{ClO_4^-}/E_{Cl^-} \quad (3)$$

2.4. Theoretical model

Electrosorption kinetics of ClO_4^- and Cl^- were quantitatively modeled using the one-dimensional dynamic CDI process model valid for batch-mode experiments which is developed based on the approach used by Porada et al. [17] and Tang et al. [24]. The ions are mainly adsorbed in electric double layers (EDLs) in the micropores (< 2 nm) of activated carbon cloths. The multi-solute solution consists of two anions (ClO_4^- and Cl^-) and one cation (Na^+). The modified Donnan (mD) model is employed to represent the EDL structure. Moreover, non-electrostatic attraction for the ions transporting into the micropores is not considered.

Based on these assumptions, the concentration of ion j in the micropores ($c_{j,mi}$) (mM) can be given by

$$c_{j,mi} = c_j \cdot \exp(-z_j \cdot \Delta\varnothing_d) \quad (4)$$

where c_j (mM) is the ion concentration outside the micropores, z_j is the ionic charge number and $\Delta\varnothing_d$ is the dimensionless Donnan potential difference (positive for the anode and negative for the cathode). Meanwhile, outside the micropores, local ion electro-neutrality is maintained, i.e.,

$$\sum_j z_j \cdot c_j = 0 \quad (5)$$

The total ion density in the micropores, $c_{ions,mi}$ (mM), is derived according to

$$c_{ions,mi} = c_{cations,mi} + c_{anions,mi} = 2 \cdot c_{Na} \cdot \cosh(\Delta\varnothing_d) \quad (6)$$

The micropore volumetric ion charge density, σ_{mi} (mM), is given by

$$\sigma_{mi} = \sum_j z_j \cdot c_{j,mi} = -2 \cdot c_{Na} \cdot \sinh(\Delta\varnothing_d) \quad (7)$$

The micropore charge density σ_{mi} relates to the Stern potential difference, $\Delta\varnothing_{st}$, according to

$$\sigma_{mi} \cdot F = -\Delta\varnothing_{st} \cdot C_{St} \cdot V_T \quad (8)$$

where F is the Faraday's constant (96,485 C mol^{-1}), C_{St} is the volumetric Stern capacity (F m^{-3}), and V_T is the thermal voltage.

In addition, we assume that the extent of ion electrosorption "per pass" is relatively low and as such, at each moment in time, the specific ion concentration throughout the cell system excluding the micropores is the same, which leads to

$$V_{mi} \frac{d\sigma_{mi}}{dt} = J \cdot A \quad (9)$$

where V_{mi} (m^3) is the micropore volume for all anodes or cathodes, and was measured to be 4.5×10^{-7} m^3 in this study. A (m^2) is the electrode projected area (either anode or cathode), and was measured to be 0.01 m^2 in this study. J (mol m^{-2} s^{-1}) is the net charge flux from

the cathode to the anode and is obtained according to

$$J = -J_{Cl} - J_{ClO4} + J_{Na} = (-D_{Cl}\cdot c_{Cl} - D_{ClO4}\cdot c_{ClO4} - D_{Na}\cdot c_{Na})\cdot L_{eff}^{-1}\cdot \Delta\varnothing_{tr} \quad (10)$$

where J_j is the flux of ion j, given by the Nernst-Planck equation, $J_j = -D_j\left(\frac{dc_j}{dX} + z_j c_j \frac{d\phi}{dX}\right)$. Note that, in this study, the concentration gradient contribution has been neglected. D_j ($m^2\,s^{-1}$) is the diffusion coefficient of ion j, L_{eff} (m) describes the total effective resistance of the spacer and both electrodes, $\Delta\varnothing_{tr}$ is the dimensionless voltage drop driving ion transport, relating to the charging voltage, V_{charge} (V), and the EDL-voltages according to

$$V_{charge}/V_T = \Delta\varnothing_{tr} + 2\,|\Delta\varnothing_{st} + \Delta\varnothing_d| \quad (11)$$

where the above equation is based on the assumption that the EDLs' structure in the anode is symmetric with that in the cathode, except for the difference in sign.

By combining Eqs. (7), (8), (10) and (11), we obtain

$$J = (-D_{Cl}c_{Cl} - D_{ClO4}c_{ClO4} - D_{Na}c_{Na})\cdot L_{eff}^{-1}\cdot\left(\frac{V_{charge}}{V_T} + 2\frac{\sigma_{mi}\cdot F}{C_{st}\cdot V_T} + 2\text{asinh}\frac{\sigma_{mi}}{2\cdot c_{Na}}\right) \quad (12)$$

In addition, the total number of moles of salt molecules in the system is conserved, i.e.,

$$V_{tot}\cdot c_{Na,0} + V_{mi}\cdot c_{ions,mi,0} = V_{tot}\cdot c_{Na} + V_{mi}\cdot c_{ions,mi} = \gamma\cdot V_{mi} \quad (13)$$

where V_{tot} (m^3) is the total water volume. Combining Eqs. (3), (4) and (10) leads to

$$c_{Na} = c_{Cl} + c_{ClO4} = \frac{\sqrt{b^2 - 4\beta(\sigma_{mi}^2 - \gamma^2)} - b}{2\beta},\ \beta = 4 - \left(\frac{V_{tot}}{V_{mi}}\right)^2,\ b = 2\gamma\frac{V_{tot}}{V_{mi}} \quad (14)$$

Finally, at time "i" (s), the following equation is satisfied,

$$J_{Cl,i}/J_{ClO4,i} = D_{Cl}\cdot c_{Cl,i}/(D_{ClO4}\cdot c_{ClO4,i}) \quad (15)$$

While at time "$i + 1$" (s),

$$c_{Cl,i+1} = (c_{Cl,i}\cdot V_{tot} - J_{Cl,i}\cdot A)/V_{tot} \quad (16)$$

$$c_{ClO4,i+1} = (c_{ClO4,i}\cdot V_{tot} - J_{ClO4,i}\cdot A)/V_{tot} \quad (17)$$

Combining Eqs. (15)–(17) leads to

$$c_{ClO4,i+1} = \frac{(C_{Cl,i+1} + C_{ClO4,i+1}) - C_{Cl,i} + D_{Cl}\cdot C_{Cl,i}/D_{ClO4}}{1 + D_{Cl}\cdot C_{Cl,i}/(D_{ClO4}\cdot C_{ClO4,i})} \quad (18)$$

Therefore, we have set up a model which could be used to quantitatively describe the electrosorption processes of perchlorate and chloride from $NaClO_4$/NaCl mixed solution by batch-mode constant-voltage CDI mode over a range of conditions. The above set of equations was numerically solved and the theoretical results were compared with the obtained experimental data.

3. Results and discussion

3.1. Effects of operating parameters and model validation

Firstly, the effects of applied voltage on the electrosorption process of ClO_4^- and NaCl were investigated. Fig. 3 shows the profiles of dynamic ClO_4^- and NaCl concentrations with time at different applied voltages (0.6 V, 0.9 V, 1.2 V) for a fixed pump flow rate of 44 mL min^{-1}, initial ClO_4^- concentration of 25 mg L^{-1} and initial NaCl concentration of 200 mg L^{-1}, from which we can see that, in the batch-mode operation, upon applying a fixed charging voltage, the ion concentration decreases rapidly and then levels off, indicating the gradual saturation of ion electrosorption on the carbon electrodes. Moreover, an increase in the applied voltage leads to a decrease in the steady-state ClO_4^- and NaCl concentrations. It is also interesting to observe that there is a strong preferential adsorption of ClO_4^- over Cl^- in the studied CDI system. This is evidenced by the significantly larger removal efficiency of ClO_4^- than that of Cl^- (Fig. 4). The removal efficiency of ClO_4^- at applied voltages of 0.6 V, 0.9 V, 1.2 V was 68%, 84%, 96%, respectively, while the removal efficiency of Cl^- at applied voltages of 0.6 V, 0.9 V, 1.2 V was 6.4%, 18%, 32%, respectively. Furthermore, the ion selectivity between ClO_4^- and Cl^- decreased with increasing applied voltages. When the applied voltage was 0.6 V and 1.2 V, the ion selectivity between ClO_4^- and Cl^- was 10.6 and 3.0, respectively. This could be explained from the fact that, when the applied voltage was high, say, 1.2 V, the steady-state ClO_4^- concentration dropped to near zero while the steady-state Cl^- concentration still remained high. It is quite reasonable to infer that, if the applied voltage further increased, the removal efficiency of ClO_4^- would show little change while the removal efficiency of Cl^- would steadily increase, thereby leading to a decreased ion selectivity between ClO_4^- and Cl^- with an increase in the applied voltage. In typical environmental scenarios, concentrations of background ions in water are usually much higher than the target contaminants as is the case in this work, and existing CDI electrodes generally have no designed selectivity towards specific contaminants. To achieve selective removal of target ions in a CDI process, certain improvements should be made for instance, coating the carbon electrode surface with a material with high selectivity towards one specific ion or synthesizing a composite electrode by mixing carbon particles with a material with high affinity towards the ion of concern [31–35]. The experimental results obtained here, however, suggest that the CDI system in this study without additional modification allowed for a favorably preferential removal of ClO_4^- over Cl^- in dual-anion solutions, which, consequently, holds great promise in the practical treatment of perchlorate-contaminated brackish water.

The model developed to describe ion electrosorption incorporated the following three categories of parameters: theoretical parameters (V_T, F), experimental parameters (V_{charge}, V_{tot}, V_{mi}, A) and fitting parameters (D_{ClO4}, D_{Cl}, D_{Na}, L_{eff}, C_{St}). We used the experimental data related to the effects of applied voltage on the electrosorption kinetics of ClO_4^- and NaCl to perform parameter fittings and got the following values: $D_{ClO4} = 9 \times 10^{-10}\,m^2\,s^{-1}$, $D_{Cl} = 1 \times 10^{-10}\,m^2\,s^{-1}$, $D_{Na} = 1 \times 10^{-10}\,m^2\,s^{-1}$, $L_{eff} = 1$ mm, $C_{St} = 5.45 \times 10^7\,F\,m^{-3}$. In such cases, it turned out that the model proposed was able to satisfactorily describe the dynamic removal processes of both ClO_4^- and NaCl at different applied voltages as can be seen from the model fits in Fig. 3, though some slight discrepancies do exist between the measured and modelling results.

We also studied the effects of other operating parameters on the electrosorption process of ClO_4^- and NaCl, including initial ClO_4^- concentration, initial NaCl concentration and pump flow rate. Meanwhile, the experimental data obtained over a range of well-defined operating conditions were used to further validate the developed model. Figs. 5 and 6 display the dynamic variation in ClO_4^- and NaCl concentrations at different initial ClO_4^- concentrations (11.25 mg L^{-1}, 25.00 mg L^{-1}, 37.00 mg L^{-1}) (initial coexisting NaCl concentration 200 mg L^{-1}) and at different initial NaCl concentrations (100 mg L^{-1}, 200 mg L^{-1}, 300 mg L^{-1}) (initial coexisting ClO_4^- concentration 25.00 mg L^{-1}), respectively, for a fixed pump flow rate of 44 mL min^{-1} and an applied voltage of 0.9 V. From Fig. 5a and 6b, it is apparent that ClO_4^- and Cl^- competed for the limited electrosorption sites because a higher initial coexisting ClO_4^- concentration led to a higher steady-state Cl^- concentration, and vice versa. From Fig. 5b and 6a, it could be observed that, when initial coexisting Cl^- (or ClO_4^-) concentration kept unchanged, a greater difference between the initial and steady-state ClO_4^- (or Cl^-) concentrations would result from a higher initial ClO_4^- (or Cl^-) concentration. The removal efficiencies of ClO_4^- and Cl^- and the ion selectivity between ClO_4^- and Cl^- under the conditions of Figs. 5 and 6 were also calculated (see Table 1). Again, results indicated that there was a significantly differential separation between ClO_4^- and Cl^- in the studied CDI system, and ClO_4^- is preferentially removed from solution over Cl^-. And we can see that the removal

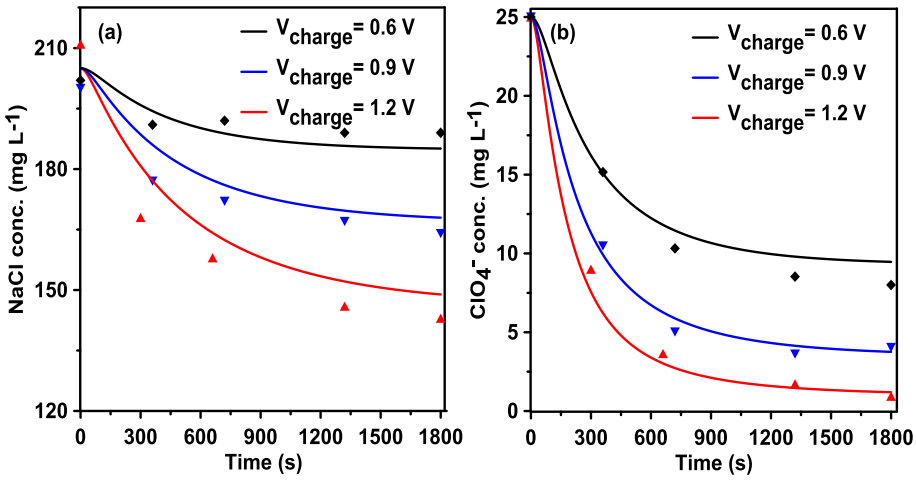

Fig. 3. Effects of charging voltage on the dynamic electrosorption processes of (a) NaCl and (b) ClO_4^-. Experimental conditions: $c_{ClO_4^-,initial}$ = 25 mg L^{-1}, $c_{NaCl,initial}$ = 200 mg L^{-1}, $\varnothing_p$ = 44 mL min^{-1} and V_{tot} = 100 mL. Symbols: experimental data; Lines: modeling results.

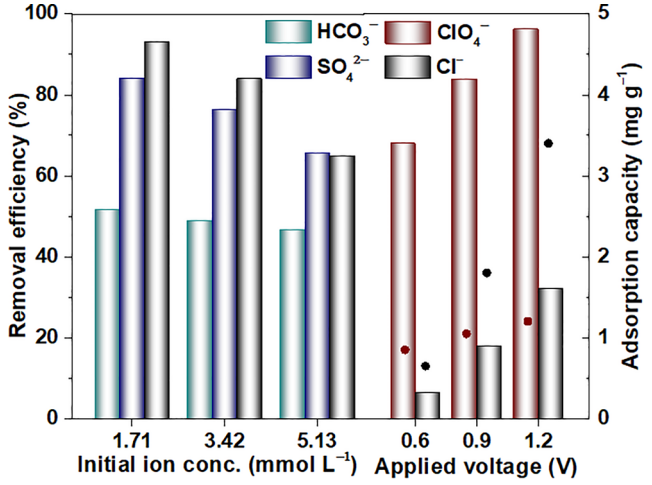

Fig. 4. Comparison of ClO_4^- removal efficiency in the presence of Cl^-, SO_4^{2-} and HCO_3^-, respectively, at the applied voltage of 0.9 V, and the removal efficiency and adsorption capacity of ClO_4^- and Cl^- in the presence of 200 mg L^{-1} NaCl under different charging voltages. Experimental conditions: $c_{ClO_4^-,initial}$ = 37 mg L^{-1}, $\varnothing_p$ = 44 mL min^{-1} and V_{tot} = 100 mL. Symbols: adsorption capacity; Bars: removal efficiency.

efficiencies of ClO_4^- and Cl^- decreased with an increase in ClO_4^- or Cl^- concentrations, while the ion selectivity between ClO_4^- and Cl^- increased with increasing ClO_4^- or Cl^- concentrations. The preferential removal of ClO_4^- over Cl^- might be caused by several reasons, e.g., larger ion diffusion coefficient of ClO_4^- than Cl^-, and/or higher affinity of the electrodes for ClO_4^- than Cl^-. However, for simplification, in the model, we attributed the selectivity between ClO_4^- and Cl^- mainly to the larger ion diffusion coefficient of ClO_4^- than Cl^-. Based on the good agreement between experimental data and theoretical results as observed from the model fits in Figs. 5 and 6, and the coefficient of determination listed in Table 1, it can be concluded that the proposed model also provides a good description of the ion removal profiles at various initial concentrations of ClO_4^- and Cl^-.

We also investigated the influence of other coexisting ions (SO_4^{2-} or HCO_3^-) which might be present in the brackish water on the removal of perchlorate by this system. The removal efficiencies of perchlorate at different initial HCO_3^-, SO_4^{2-} or Cl^- concentrations (1.71 mM, 3.42 mM, 5.13 mM) were summarized in the left part of Fig. 4, from which we can see that, under the same initial ion concentrations, HCO_3^- had a much greater influence on perchlorate removal than SO_4^{2-} and Cl^-, while the effects of SO_4^{2-} and Cl^- on perchlorate removal were roughly similar. Additionally, with an increase in the initial ion concentrations, perchlorate removal efficiency in the presence of SO_4^{2-} decreased obviously with the trend consistent

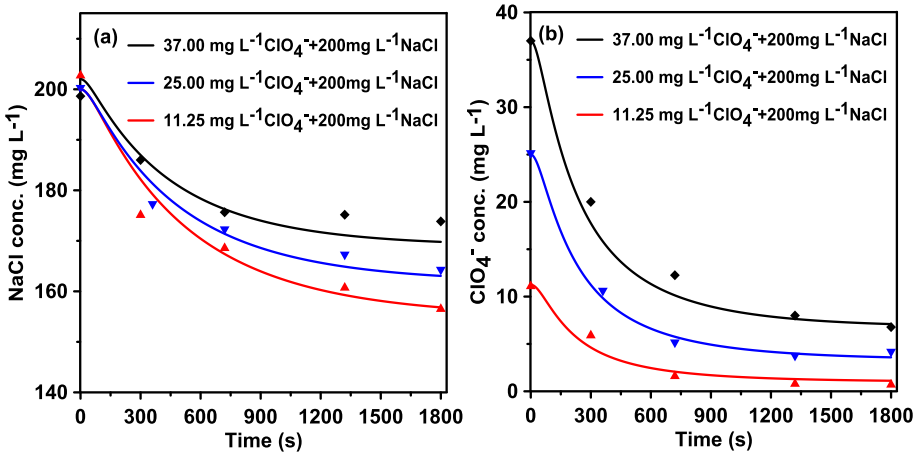

Fig. 5. Effects of initial ClO_4^- concentrations on the dynamic electrosorption processes of (a) NaCl and (b) ClO_4^- with initial coexisting NaCl concentration kept at 200 mg L^{-1}. Experimental conditions: V_{charge} = 0.9 V, $\varnothing_p$ = 44 mL min^{-1} and V_{tot} = 100 mL. Symbols: experimental data; Lines: modeling results.

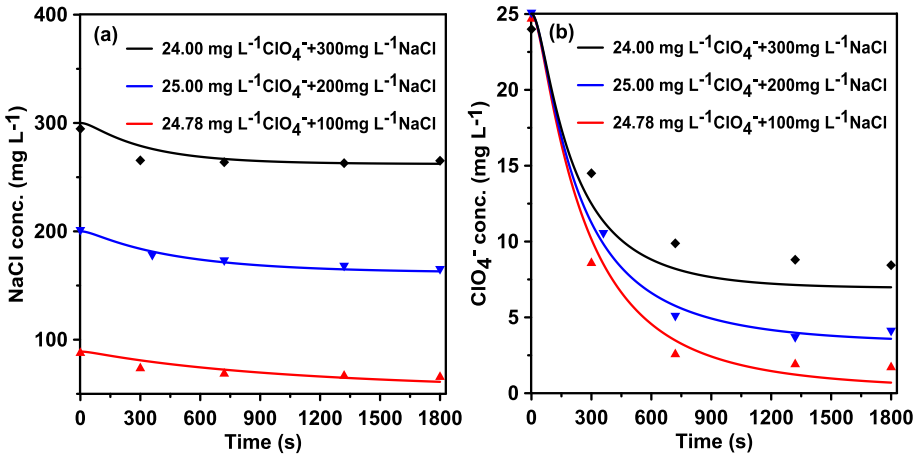

Fig. 6. Effects of initial NaCl concentrations on the dynamic electrosorption processes of (a) NaCl and (b) ClO_4^- with initial coexisting ClO_4^- concentration kept at approximately 25 mg L^{-1}. Experimental conditions: V_{charge} = 0.9 V, $\varnothing_p$ = 44 mL min^{-1} and V_{tot} = 100 mL. Symbols: experimental data; Lines: modeling results.

Table 1
Ion selectivity between ClO_4^- and Cl^-, adsorption capacity, charge efficiency and coefficient of determination (R^2) of the model fits for ClO_4^- and Cl^- under various conditions.

($c_{ClO_4^-,initial}$, $c_{NaCl,initial}$) (mg L^{-1})	Voltage (V)	$S_{ClO_4^-/Cl^-}$	$Q_{ClO_4^-}$(mg g^{-1})	Q_{Cl^-}(mg g^{-1})	Charge efficiency (%)	R^2 (ClO_4^-)	R^2 (Cl^-)
(25.00, 200)	0.6	10.57	0.85	0.39	62.70	0.975	0.676
	0.9	4.66	1.05	1.09	65.76	0.996	0.971
	1.2	2.99	1.20	2.06	70.41	0.980	0.930
(11.00, 200)	0.9	4.06	0.52	1.40		0.972	0.957
(25.00, 200)		4.66	1.05	1.09	65.76	0.996	0.971
(37.00, 200)		6.54	1.51	0.75		0.984	0.907
(25.00, 100)		3.73	1.15	0.67	68.42	0.988	0.776
(25.00, 200)		4.66	1.05	1.09	65.76	0.996	0.971
(25.00, 300)		6.48	0.78	0.89	55.50	0.931	0.752

with that in the presence of Cl^-, while perchlorate removal efficiency in the presence of HCO_3^- only showed a small decrease.

Fig. 7 shows ClO_4^- and Cl^- electrosorption processes as a function of pump flow rate. The effect of pump flow rate on the ClO_4^- and Cl^- electrosorption can be considered negligible for the studied three different flow rates. This is in agreement with the theoretical model. In fact, in our model, the parameter of flow rate is not included. We assumed that, the extent of ion electrosorption "per pass" is relatively low, and as such, at each moment in time, the specific ion concentration throughout the cell system (i.e., electrode macropores, spacer channel, pipes and recycling vessel) is the same. This implicitly determines a lack of effect of flow rate on ion removal in the theoretical part. From the perspective of energy consumption, a lower flow rate means a lower pumping energy requirement, and hence is favorable to the system optimization on the premise that it has little influence on the ion electrosorption. However, it is worth noting that the flow rate should not be too low, otherwise the continuous ion removal would be impeded and dead zones would be created in the spacer region resulting in compromised performance. It is also worth noting that batch-mode CDI operation and single-pass CDI operation respond differently to the flow

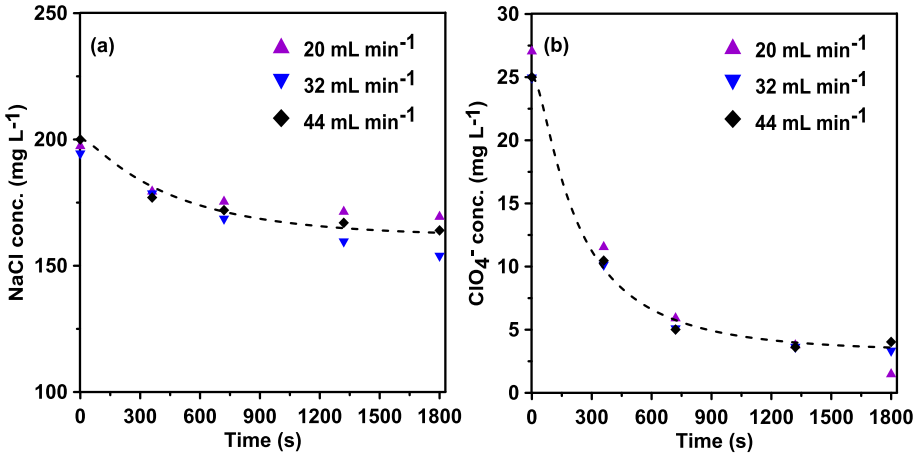

Fig. 7. Effects of pump flow rate on the dynamic electrosorption processes of (a) NaCl and (b) ClO_4^-. Experimental conditions: $c_{ClO_4^-,initial}$ = 25 mg L^{-1}, $c_{NaCl,initial}$ = 200 mg L^{-1}, V_{charge} = 0.9 V and V_{tot} = 100 mL. Symbols: experimental data; Lines: modeling results.

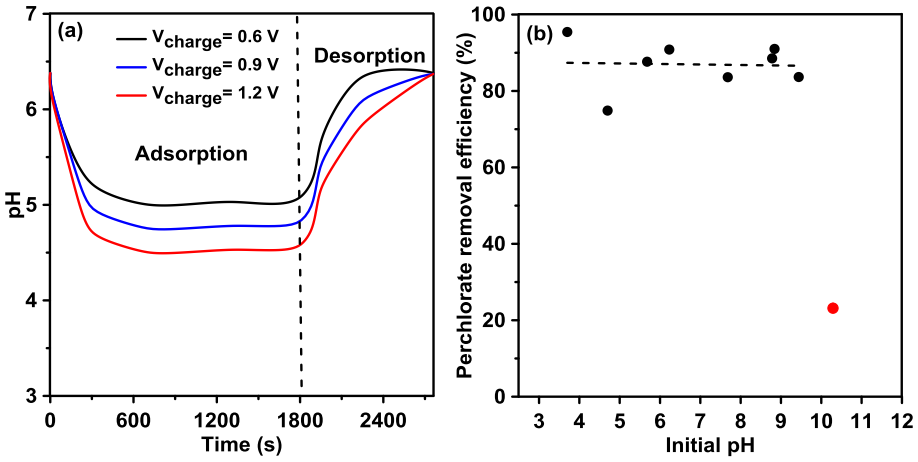

Fig. 8. (a) pH variation during adsorption and desorption steps under different charging voltages with initial pH unadjusted, (b) Effects of initial pH on ClO_4^- removal during electrosorption process at the applied voltage of 0.9 V. Experimental conditions: $c_{ClO_4^-,initial}$ = 37 mg L^{-1}, $c_{NaCl,initial}$ = 200 mg L^{-1}, $\varnothing_p$ = 44 mL min^{-1}, $V_{discarge}$ = 0 V and V_{tot} = 100 mL.

rate. In single-pass operation, the effluent ion concentrations versus time are greatly affected by the flow rate, and a lower minimum effluent ion concentration would be obtained on decreasing the flow rate as a result of the greater residence time of the solution in the CDI cell [27].

In addition to the effects of operating parameters on ClO_4^- and Cl^- electrosorption, pH fluctuation also needs consideration as pH represents an important water quality indicator. Fig. 8a depicts the pH variation in the whole cycle (adsorption and desorption) under different charging voltages. It was found that the pH decreased quickly and then tended to be stable during adsorption, followed by a gradual increase to the initial value during desorption. These profiles of pH variation are quite similar to those reported by Tang et al. [36], and could be attributed to the Faradaic reactions occurring on the surfaces of and/or within carbon electrodes. The pH fluctuations when the CDI cell was charged at a voltage of 0.6 − 1.2 V were insignificant and within the pH range of 4.5–6.5, implying that the change of pH exerted an insignificant influence on the treated water quality and ion removal during the batch-mode CDI operation. Fig. 8b shows the effect of initial pH (from 3.7 ± 0.1 to 10.3 ± 0.1) on the removal efficiency of ClO_4^-. As can be seen, the removal efficiency of ClO_4^- fluctuated between 75% and 91% over the initial pH range of 3.7–9.4, but got low at strongly alkaline pH of 10.3. In the strongly alkaline solution, the concentration of OH^- is relatively high and OH^- would compete with ClO_4^- for the limited sorption sites. Therefore, the initial pH should not be too high, otherwise the ClO_4^- electrosorption would be impeded. There is no need to adjust the initial pH for treating the perchlorate-contaminated brackish water.

3.2. Charge efficiency, operational stability and effects of NOM

Fig. 9 displays the variation of current at different applied voltages of 0.6 V, 0.9 V, 1.2 V, and at different initial coexisting NaCl concentrations (100 mg L^{-1}, 200 mg L^{-1}, 300 mg L^{-1}). We can see that the current declines rapidly at the charging beginning and then decreases slowly until saturation of the electrode capacity. At higher applied charging voltage, more charge flows into the cell, while initial coexisting NaCl concentrations have insignificant influence on the charge amount flowing into the cell. The charge efficiency (Λ) can be calculated according to $\Lambda = \Gamma/\Sigma$, where Γ (mmol) represents the sum of measured equilibrium $NaClO_4$ and NaCl adsorbed amount during charging, Σ (mmol) represents the total charge transferred during charging. Σ (mmol) can be derived by integrating the current vs. time and being divided by the Faraday's constant (F = 96,485 C mol^{-1}). The charge efficiency in the CDI cell at different charging voltages and different initial coexisting NaCl concentrations is summarized in Table 1, suggesting that Λ is below unity and generally increases with increasing charging voltage (0.6 − 0.9 V) and decreases with increasing initial coexisting NaCl concentrations. The results are also consistent with other investigations [27,29,30].

Adsorption-desorption cycles were conducted to evaluate the regeneration of electrodes and operational stability of the CDI cell. Fig. 10a shows the dynamic variation in ClO_4^- concentration over five consecutive cycles. As can be seen, almost all ClO_4^- ions electrosorbed during charging could be released from the electrodes during discharging, which suggests that the electrodes have good regeneration performance during ClO_4^- removal process in the presence of NaCl. Moreover, no significant discrepancy between the previous cycle and the following cycle is observed in the profiles of ClO_4^- concentration versus time, which indicates that the cell provided good reproducibility over a small number of successive runs. In addition, only a small decrease in performance of the CDI cell over the course of several months of intermittent operation was observed, as indicated by Fig. 10b.

On the basis of the adsorption-desorption cycles, we further investigated the effect of NOM on ClO_4^- removal in the presence of NaCl by adding certain amount of sodium humate into the solution with an initial total organic carbon (TOC) concentration of 12.6 mg L^{-1}, and the results are presented in Fig. 10a. In the first cycle, the ClO_4^- concentration dropped from 37 mg L^{-1} to 12 mg L^{-1} in the constant-voltage adsorption step, and then recovered to approximately 34 mg L^{-1} in the short-circuiting desorption step. In the following cycles, the ClO_4^- concentrations at the end of adsorption and desorption are similar to those in the first cycle. The notable decline in the ClO_4^- removal ability of the CDI cell in the presence of NOM could be explained from two aspects: 1) Driven by electrical field, the negatively charged organic compounds in the solution would move towards the carbon electrodes and compete with ClO_4^- for available adsorption sites; 2) some humics are adsorbed on the surface of carbon electrodes by chemical adsorption and hydrophobic interaction thereby resulting in the occupation of adsorption sites and these compounds often could not be efficiently desorbed during the regeneration cycle. This is evidenced by the fact that, at the end of desorption, only 9.7 mg L^{-1} TOC existed in the solution indicating that 2.9 mg L^{-1} TOC were retained in the electrodes. 3) Dissolved organics with large molecular weight and size might block the pores of the electrodes and inhibit ClO_4^- from reaching adsorption sites. This is confirmed by the result that the BET specific surface area of the electrode in the presence of NOM at the end of electrosorption is 642 m^2 g^{-1}, 42.6% lower than that of the initial electrode in the absence of NOM. Furthermore, the phenomena observed here were consistent with those of previous studies by Gabelich et al. [37], Zhang

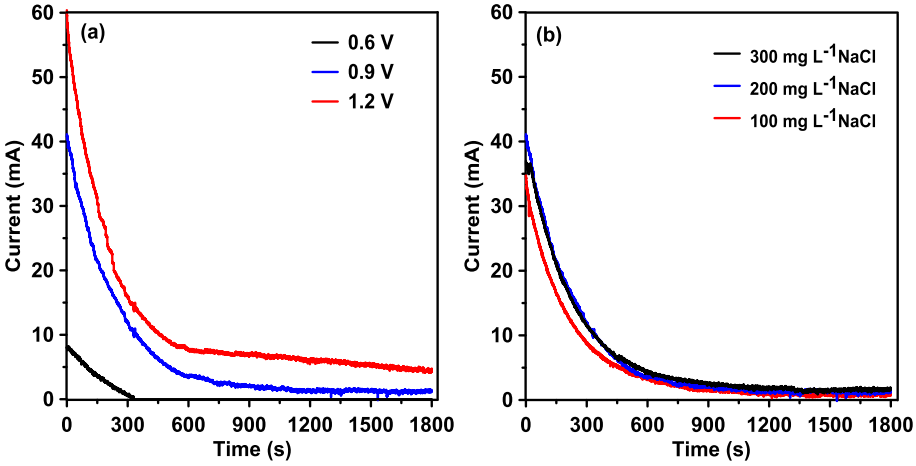

Fig. 9. Variation of current during charging in the CDI cell at different (a) charging voltages and (b) initial coexisting NaCl concentrations.

et al. [38], Wang et al. [39] and Chen et al. [40] who found that the presence of NOM might foul the carbon electrodes and have negative impacts on ion removal. The results suggested the necessity of a pretreatment to reduce the presence of NOM for the sustainable operation of CDI, whereby broadening the potential application fields.

3.3. CDI cells in parallel

In the previous sections, only one pair of electrodes (one cell) was used. To improve the ion removal performance or increase the volume of treated water for practical applications, many cells can be pressed together in parallel with regard to fluid flow and power charging to construct a stack. We set up a stack with seven pairs of electrodes (each electrode projected area is 8 cm × 8 cm), and in this section, ClO_4^- and Cl^- electrosorption processes between this stack and one CDI cell (the electrode projected area is also 8 cm × 8 cm) were compared. The modeling results were also presented to further verify its appropriateness.

As can be seen from Fig. 11, the CDI stack had a much more superior ion removal performance than one CDI cell under the same operating conditions. The removal efficiencies of ClO_4^- and Cl^- in the CDI cell were 13% and 1%, respectively, while the removal efficiencies of ClO_4^- and Cl^- in the CDI stack reached 59% and 11%, respectively. Additionally, the theoretical model developed adequately describes the experimental results and shows how change in the selected system design and operating conditions may impact treated water quality. As a matter of fact, the ultimate aim of CDI modeling is to derive mathematical expressions that not just describe previously recorded data, but also enable prediction of CDI performance under various possible design and operational scenarios. The validated model in this study appears to be a useful tool for quantitative description and prediction of the electrosorption processes of both ClO_4^- and Cl^- over a range of operating conditions, cell arrangements and feed water compositions.

4. Conclusions

In this study, we have examined, both experimentally and theoretically, the feasibility of ClO_4^- removal from brackish water by batch-mode constant-voltage CDI system. In the aspect of experiments, effects of various operational parameters (e.g., applied charging voltage, initial pH, initial ClO_4^-, Cl^-, HCO_3^-, and SO_4^{2-} concentrations, and pump flow rate) on the dynamic electrosorption processes of both ClO_4^- and Cl^- were studied with the results showing that 1) a higher applied voltage (ranging from 0.6 V to 1.2 V) favorably led to a decrease in the lowest ClO_4^- and Cl^- concentrations; 2) ClO_4^- and Cl^- competed, to a certain extent, for the limited electrosorption sites. HCO_3^- had a much greater influence on ClO_4^- removal than SO_4^{2-} and Cl^-, while the effects of SO_4^{2-} and Cl^- on ClO_4^- removal were roughly similar; 3) pump flow rate had little influence on the ClO_4^- and Cl^- electrosorption kinetics within limits; 4) a favorably strong preferential

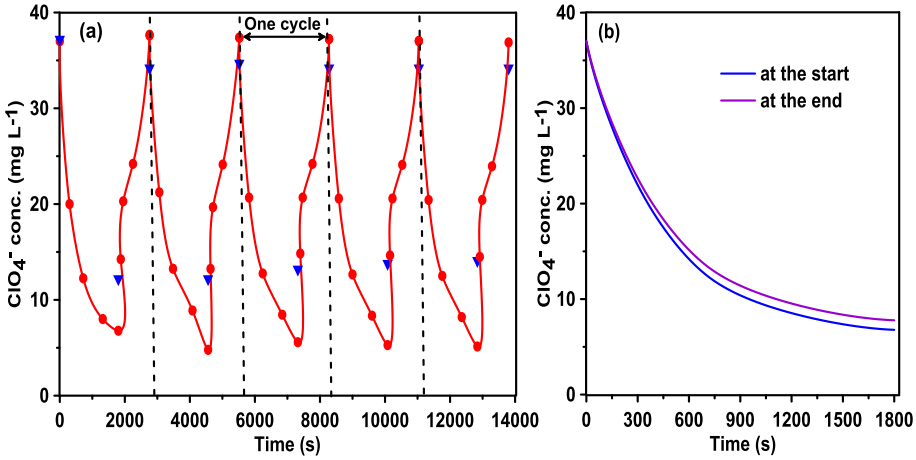

Fig. 10. (a) Dynamic variation in ClO_4^- concentration over five consecutive cycles in the absence of NOM (red line) and in the presence of NOM (blue triangle), (b) The difference in performance of the CDI cell at the start and at the end during the several months of intermittent operation in the absence of NOM. Experimental conditions: $c_{ClO_4^-,initial}$ = 37 mg L^{-1}, $c_{NaCl,initial}$ = 200 mg L^{-1}, $\varnothing_p$ = 44 mL min^{-1}, V_{charge} = 0.9 V, $V_{discarge}$ = 0 V and V_{tot} = 100 mL.

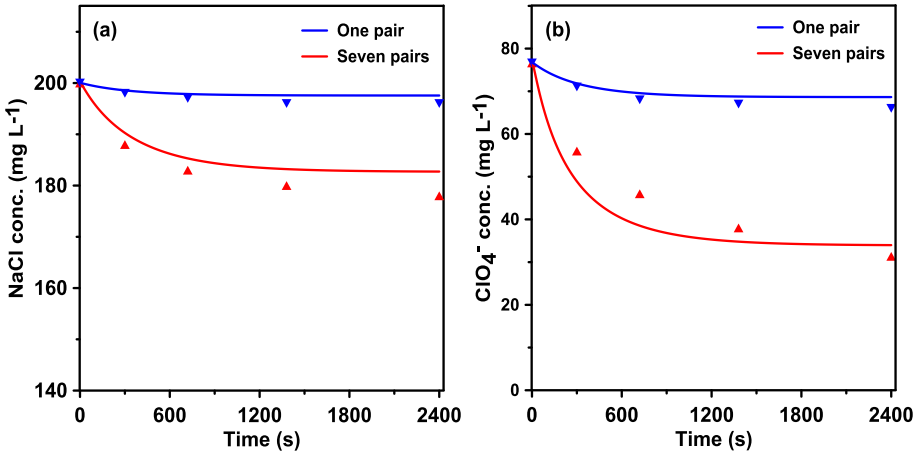

Fig. 11. Comparison of (a) NaCl and (b) ClO_4^- electrosorption processes between the CDI stack with seven pairs of electrodes and the CDI cell with only one pair of electrodes. Experimental conditions: $c_{ClO_4^-,initial}$ = 76 mg L^{-1}, $c_{NaCl,initial}$ = 200 mg L^{-1}, $\varnothing_p$ = 44 mL min^{-1}, V_{charge} = 0.9 V, $V_{discarge}$ = 0 V and V_{tot} = 700 mL. Symbols: experimental data; Lines: modeling results.

adsorption of ClO_4^- over Cl^- occurred under various conditions and the ion selectivity between ClO_4^- and Cl^- varied with the operational parameters. Adsorption-desorption cycles and the small decrease in performance of the CDI cell over the course of several months of intermittent operation suggested the good regeneration of electrodes and operational stability of the CDI cell. The notable decline in the ClO_4^- removal ability of the CDI cell in the presence of relatively high level of NOM suggested the necessity of a pre-treatment to reduce the presence of NOM for the sustainable operation of CDI. The scale-up studies indicated that the CDI stack assembled with multiple pairs of electrodes could achieve a much more superior ion removal performance compared to the CDI cell with only one pair of electrodes. In the aspect of theory, the proposed model provided a good quantitative description of the ClO_4^- and Cl^- removal profiles over a range of operating conditions, cell arrangements and feed water compositions. The validated model is expected to have an important role to play in establishing CDI as a viable treatment technology for perchlorate-contaminated brackish water.

Acknowledgements

This study was financially supported by the National Natural Science Foundation of China (51809088, 51679082, 51479072, 51521006, 51579094), the Hunan Science and Technology Innovation Program of China (2018RS3037), the Fundamental Research Funds for the Central Universities, China (531107051072) and the Science and Technology Plan Project of Hunan Province, China (No. 2018SK2047).

References

[1] R. Nerenberg, B.E. Rittmann, Hydrogen-based, hollow-fiber membrane biofilm reactor for reduction of perchlorate and other oxidized contaminants, Water Sci. Technol. 49 (2004) 223–230.
[2] F. Yao, Y. Zhong, Q. Yang, et al., Effective adsorption/electrocatalytic degradation of perchlorate using Pd/Pt supported on N-doped activated carbon fiber cathode, J. Hazard. Mater. 323 (2016) 602–610.
[3] S.J. Stetson, R.B. Wanty, D.R. Helsel, et al., Stability of low levels of perchlorate in drinking water and natural water samples, Anal. Chim. Acta 567 (2006) 108–113.
[4] D.C. Herman, W.T. Frankenberger, Bacterial reduction of perchlorate and nitrate in Water, J. Environ. Qual. 28 (1999) 1018–1024.
[5] Q. Yang, F. Yao, Y. Zhong, et al., Catalytic and electrocatalytic reduction of perchlorate in water – A review, Chem. Eng. J. 306 (2016) 1081–1091.
[6] R. Srinivasan, G.A. Sorial, R. Srinivasan, Treatment of perchlorate in drinking water: a critical review, Sep. Purif. Technol. 69 (2009) 7–21.
[7] L. Ye, H. You, J. Yao, et al., Water treatment technologies for perchlorate: a review, Desalination 298 (2012) 1–12.
[8] N. Bardiya, J.H. Bae, Dissimilatory perchlorate reduction: a review, Microbiol. Res. 166 (2011) 237–254.
[9] J. Guo, J. Liang, X. Yuan, et al., Efficient visible-light driven photocatalyst, silver (meta) vanadate: synthesis, morphology and modification, Chem. Eng. J. 352 (2018) 782–802.
[10] L. Jiang, X. Yuan, G. Zeng, et al., In-situ synthesis of direct solid-state dual Z-scheme $WO_3/g\text{-}C_3N_4/Bi_2O_3$ photocatalyst for the degradation of refractory pollutant, Appl. Catal. B Environ. 227 (2018) 376–385.
[11] E.T. Urbansky, M.R. Schock, Issues in managing the risks associated with perchlorate in drinking water, J. Environ. Manage. 56 (1999) 79–95.
[12] J.K. Choe, M.H. Mehnert, J.S. Guest, et al., Comparative assessment of the environmental sustainability of existing and emerging perchlorate treatment technologies for drinking water, Environ. Sci. Technol. 47 (2013) 4644–4652.
[13] M.A. Anderson, A.L. Cudero, J. Palma, Capacitive deionization as an electrochemical means of saving energy and delivering clean water. Comparison to present desalination practices: will it compete? Electrochim. Acta 55 (2010) 3845–3856.
[14] S. Porada, B.B. Sales, H.V. Hamelers, et al., Water desalination with wires, J. Phys. Chem. L 3 (2012) 1613–1618.
[15] M.E. Suss, S. Porada, X. Sun, et al., Water desalination via capacitive deionization: what is it and what can we expect from it? Energy Environ. Sci. 8 (2015) 2296–2319.
[16] A. Subramani, J.G. Jacangelo, Emerging desalination technologies for water treatment: a critical review, Water Res. 75 (2015) 164–187.
[17] S. Porada, R. Zhao, A.V.D. Wal, et al., Review on the science and technology of water desalination by capacitive deionization, Prog. Mater Sci. 58 (2013) 1388–1442.
[18] W.W. Tang, J. Liang, D. He, et al., Various cell architectures of capacitive deionization. Recent advances and future trends, Water Res. 150 (2019) 225–251.
[19] C. Zhang, D. He, J. Ma, et al., Faradaic reactions in capacitive deionization (CDI) – problems and possibilities: a review, Water Res. 128 (2018) 314–330.
[20] M. Mossad, L. Zou, A study of the capacitive deionisation performance under various operational conditions, J. Hazard. Mater. 213–214 (2012) 491–497.
[21] C. Tan, C. He, W. Tang, et al., Integration of photovoltaic energy supply with membrane capacitive deionization (MCDI) for salt removal from brackish waters, Water Res. 147 (2018) 276–286.
[22] E. Avraham, M. Noked, A. Soffer, et al., The feasibility of boron removal from water by capacitive deionization, Electrochim. Acta 56 (2011) 6312–6317.
[23] G.-H. Huang, T.-C. Chen, S.-F. Hsu, et al., Capacitive deionization (CDI) for removal of phosphate from aqueous solution, Desalin. Water Treat. 52 (2014) 759–765.
[24] W. Tang, P. Kovalsky, D. He, et al., Fluoride and nitrate removal from brackish groundwaters by batch-mode capacitive deionization, Water Res. 84 (2015) 342–349.
[25] X. Huang, D. He, W. Tang, et al., Investigation of pH-dependent phosphate removal from wastewaters by membrane capacitive deionization (MCDI), Environ. Sci. Water Res. Technol. 3 (2017) 875–882.
[26] W. Tang, D. He, C. Zhang, et al., Optimization of sulfate removal from brackish water by membrane capacitive deionization (MCDI), Water Res. 121 (2017) 302–310.
[27] W. Tang, P. Kovalsky, B. Cao, et al., Investigation of fluoride removal from low-salinity groundwater by single-pass constant-voltage capacitive deionization, Water Res. 99 (2016) 112–121.
[28] L. Jie, G.M. Zeng, S.L. Guo, et al., Uncertainty analysis of stochastic solute transport in a heterogeneous aquifer, Environ. Eng. Sci. 26 (2009) 359–368.
[29] P.M. Biesheuvel, S. Porada, M. Levi, et al., Attractive forces in microporous carbon electrodes for capacitive deionization, J. Solid State Electrochem. 18 (2014) 1365–1376.
[30] T. Kim, J.E. Dykstra, S. Porada, et al., Enhanced charge efficiency and reduced energy use in capacitive deionization by increasing the discharge voltage, J. Colloid Interface Sci. 446 (2015) 317–326.
[31] K. Zuo, J. Kim, A. Jain, et al., Novel composite electrodes for selective removal of sulfate by the capacitive deionization process, Environ. Sci. Technol. 52 (2018) 9486–9494.

[32] D.H. Lee, T. Ryu, J. Shin, et al., Selective lithium recovery from aqueous solution using a modified membrane capacitive deionization system, Hydrometallurgy 173 (2017) 283–288.
[33] Y. Liu, W. Ma, Z. Cheng, et al., Preparing CNTs/Ca-Selective zeolite composite electrode to remove calcium ions by capacitive deionization, Desalination 326 (2013) 109–114.
[34] X. Su, T.A. Hatton, Redox-electrodes for selective electrochemical separations, Adv. Colloids Interface 244 (2016) 6–20.
[35] J. Liang, X. Li, Z. Yu, et al., Amorphous MnO_2 modified biochar derived from aerobically composted swine manure for adsorption of Pb (II) and Cd (II), ACS Sustainable Chem. Eng. 5 (2017) 5049–5058.
[36] W. Tang, H. Di, C. Zhang, et al., Comparison of Faradaic reactions in capacitive deionization (CDI) and membrane capacitive deionization (MCDI) water treatment processes, Water Res.. 120 (2017) 229–237.
[37] C.J. Gabelich, T.D. Tran, I.H.M. Suffet, Electrosorption of inorganic salts from aqueous solution using carbon aerogels, Environ. Sci. Technol.. 36 (2002) 3010–3019.
[38] W. Zhang, M. Mohamed, L. Zou, A study of the long-term operation of capacitive deionisation in inland brackish water desalination, Desalination 320 (2013) 80–85.
[39] C. Wang, H. Song, Q. Zhang, et al., Parameter optimization based on capacitive deionization for highly efficient desalination of domestic wastewater biotreated effluent and the fouled electrode regeneration, Desalination 365 (2015) 407–415.
[40] L. Chen, C. Wang, S. Liu, et al., Investigation of the long-term desalination performance of membrane capacitive deionization at the presence of organic foulants, Chemosphere 193 (2018) 989–997.